

**PCASP Measurements and Data Processing****(Addendum: 20200822)****Jeff Snider, Shelby Fuller, and Matt Burkhardt**

**University of Wyoming  
Department of Atmospheric Science  
Laramie, WY**

After BBFLUX two Wyoming PCASPs were intercompared. An analysis of results from the intercomparison flight are in the PCASP report ([http://www-das.uwyo.edu/~jsnider/pcasp\\_measurement\\_processing\\_v2.pdf](http://www-das.uwyo.edu/~jsnider/pcasp_measurement_processing_v2.pdf)). More analysis of that flight is provided here. The two PCASPs are distinguished as PCASP-2 = SN39798-0200-26 and PCASP-1 = SN1013-0502-29. As described in the PCASP report, the PCASP-1/PCASP-2 intercomparison data were acquired inside a wildfire plume. In this analysis, no correction of aerosol refractive index or of particle coincidence was applied. However, the lowest three channels of PCASP-2 were discarded. Excessive noise associated with those channels is the reason for omitting those data. Noise in channels 1 to 3 is not evident in PCASP-2 BBFLUX measurements that we have analyzed, but that does not exclude the possibility of noise affecting the larger quantity of BBFLUX PCASP-2 data analyzed by our colleague Min Deng. This issue is discussed below. The following table has the date interval for the PCASPs flown on the King Air during BBFLUX, and the date of the intercomparison flight.

Date	PCASP	Serial Number
20180721 to 20180812	PCASP-2	39798-0200-26
20180819 to 20180917	PCASP-1	1013-0502-29
20180928	PCASP-1 and PCASP-2 intercompared on King Air	

Figures 1a - b and Figs. 2a - b have aerosol size distributions and aerosol surface area distributions, from PCASP-1 and PCASP-2, during the intercomparison flight. The distributions were selected from the same 9 second interval shown in Fig. 5 of the PCASP report. This PCASP intercomparison reveals the following:

- 1) Aerosol concentration is 11% larger for the PCASP-2
- 2) Aerosol surface area is 69% larger for PCASP-2
- 3) The N-to-S ratio ( $\langle N \rangle / \langle S \rangle$ ) is smaller for PCASP-2 ( $\langle N \rangle / \langle S \rangle = 5 \mu\text{m}^{-2}$ ) compared to PCASP-1 ( $\langle N \rangle / \langle S \rangle = 9 \mu\text{m}^{-2}$ )

In addition, graphs of size-integrated aerosol concentration (N) versus size-integrated aerosol surface area (S), as in Min Deng's analysis, were analyzed. Scatterplots of N versus S were plotted for six BBFLUX plumes. Results shown in Fig. 3c and Fig. 4c were acquired using PCASP-1 (20180915) and PCASP-2 (20180812), respectively. The scatterplots of N versus S (Fig. 3c and Fig. 4c) represent exceptions to the finding of Min Deng who showed that the y intercept is less than or equal to  $\log_{10}(N) = 2.6$  for measurements made with PCASP-1 and greater than  $\log_{10}(N) = 2.6$  for measurements made with PCASP-2. In contrast to the relatively small subset of BBFLUX data we analyzed, Min Deng's analysis of BBFLUX PCASP-2 and PCASP-1 data was based on measurements aggregated from the  $< 20180818$  and  $> 20180818$  subsets of the campaign.

### Summary –

Min Deng presented measurements of aerosol concentration and aerosol surface area from BBFLUX. Her N versus S scatterplots were conditioned on the PCASP used to make the measurements. Prior to 20180818, measurements were made using PCASP-2. After 20180818, measurements were made using PCASP-1. A systematic shift of the aerosol size distribution, and notably, a shift to larger second moment and a shift to larger third moment, in measurements made with PCASP-1, are evident in Min Deng's analysis. This suggests that the change from PCASP-2 to PCASP-1, made during BBFLUX, is at least partially responsible for the shift Min Deng shows in her PCASP scatterplots. Atmospheric factors may have also contributed to the shift she documents.

Additionally, we have also presented N versus S scatterplots for two BBFLUX plumes. One plume was monitored using PCASP-1 (Figs. 3a – c), and one was monitored using PCASP-2 (Figs. 4a – c). The N versus S scatterplots for these plumes deviate from Min Deng's conditional scatterplots. Notably, the y intercepts in the N versus S scatterplots (Figs. 3c and 4c) deviate from the general tendency that Min Deng shows in her conditional scatterplots.

With regard to measurements from the PCASP intercomparison flight, there are three relevant findings. First, the N-to-S ratio ( $\langle N \rangle / \langle S \rangle$ ) is smaller for measurements made with PCASP-2. This seems contrary to what is seen in Min Deng's conditional scatterplots but this observation could have been, at least partially, a consequence of atmospheric changes (e.g., a difference in plume age during the intercomparison vs the average plume age in Min Deng's data set). Second, the size distribution reported by PCASP-2 has a sharp peak (at  $\sim 0.3 \mu\text{m}$ ), and in contrast, the PCASP-1 distribution is smoother (c.f., Figs. 1a – b and Figs. 2a - b). Third, during the intercomparison flight the PCASP-2 data had noise associated with the lowest three size channels of the distribution. Those channels were removed from the

analysis of intercomparison measurements presented here. However, noise in channels 1 to 3 is not evident in PCASP-2 BBFLUX data that we have analyzed.

In sum, it is our opinion is that PCASP-1 measurements can be used to develop correlations among lidar extinction and PCASP-derived moments. PCASP-2 measurements can also be used for this, but because that instrument experienced a hardware failure during BBFLUX, and because of issues associated with PCASP-2 after it was repaired and tested during the intercomparison, we are cautious of PCASP-2 measurements made during BBFLUX. Further, we are not confident how to correct for bias in PCASP-2 measurements made during BBFLUX. Whether or not a bias exists in those data is conjectural. Using the intercomparison flight result to do a correction may not be the way to proceed because there is suspicion that those PCASP-2 measurements are not representative of how the instrument was operating during BBFLUX.

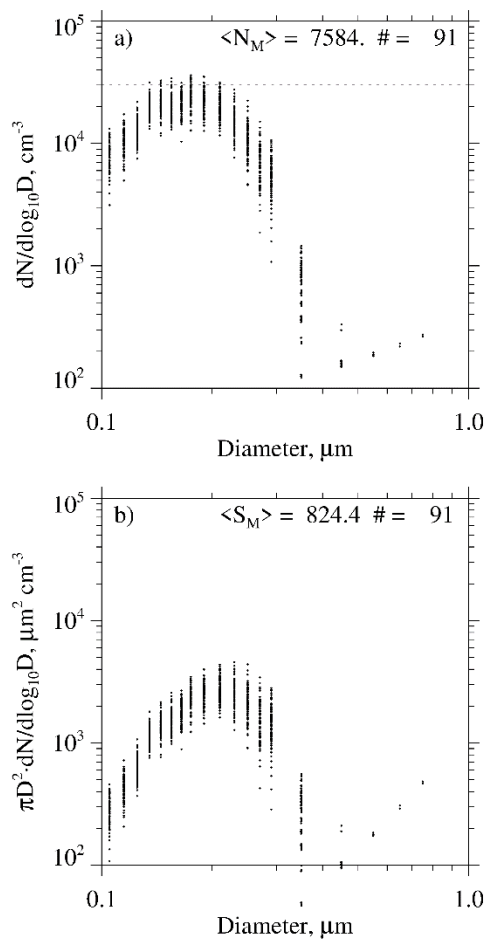


Figure 1 – PCASP-1 measurements from the intercomparison flight (20180928). a)  $dN/d\log D$  from the 9 s data segment indicated by dashed vertical lines in Fig. 5 of the report. b)  $dS/d\log D$  from the 9 s data segment indicated by dashed vertical lines in Fig. 5 of the report.

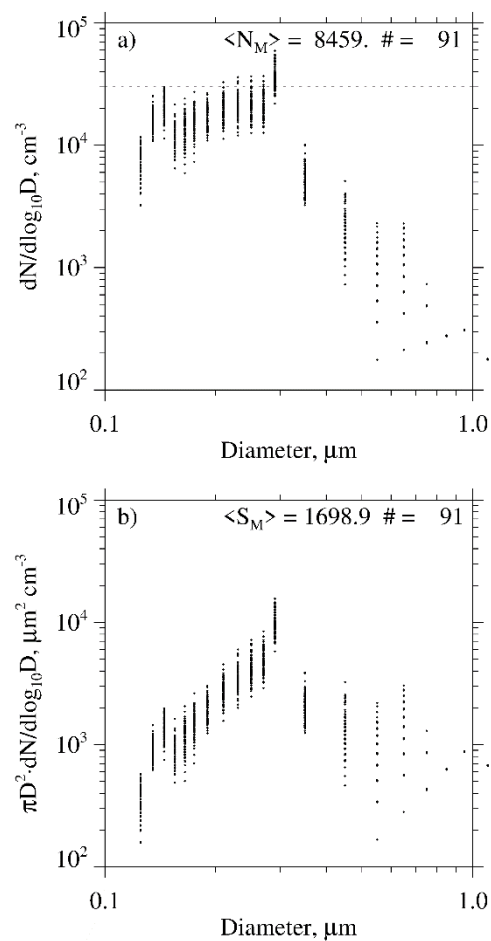


Figure 2 – PCASP-2 measurements from the intercomparison flight (20180928). a)  $dN/d\log D$  from the 9 s data segment indicated by dashed vertical lines in Fig. 5 of the report. b)  $dS/d\log D$  from the 9 s data segment indicated by dashed vertical lines in Fig. 5 of the report.

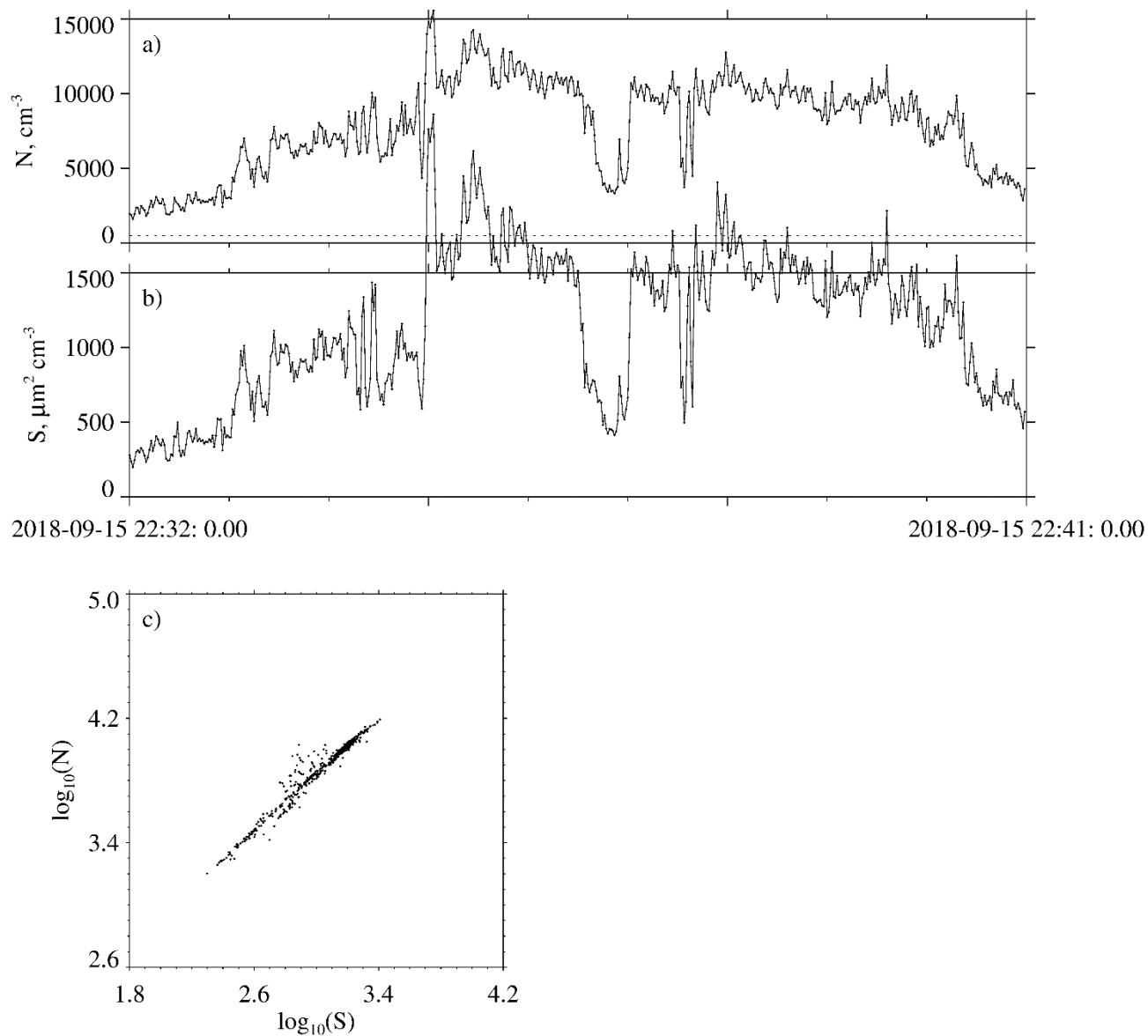


Figure 3 – Wildfire plume measurements made on 20180915 using PCASP-1. a) 9 min sequence of size-integrated aerosol concentration. b) 9 min sequence of size-integrated aerosol surface. c) N versus S scatterplot of values acquired during the 9 min sequence shown in the upper two panels.

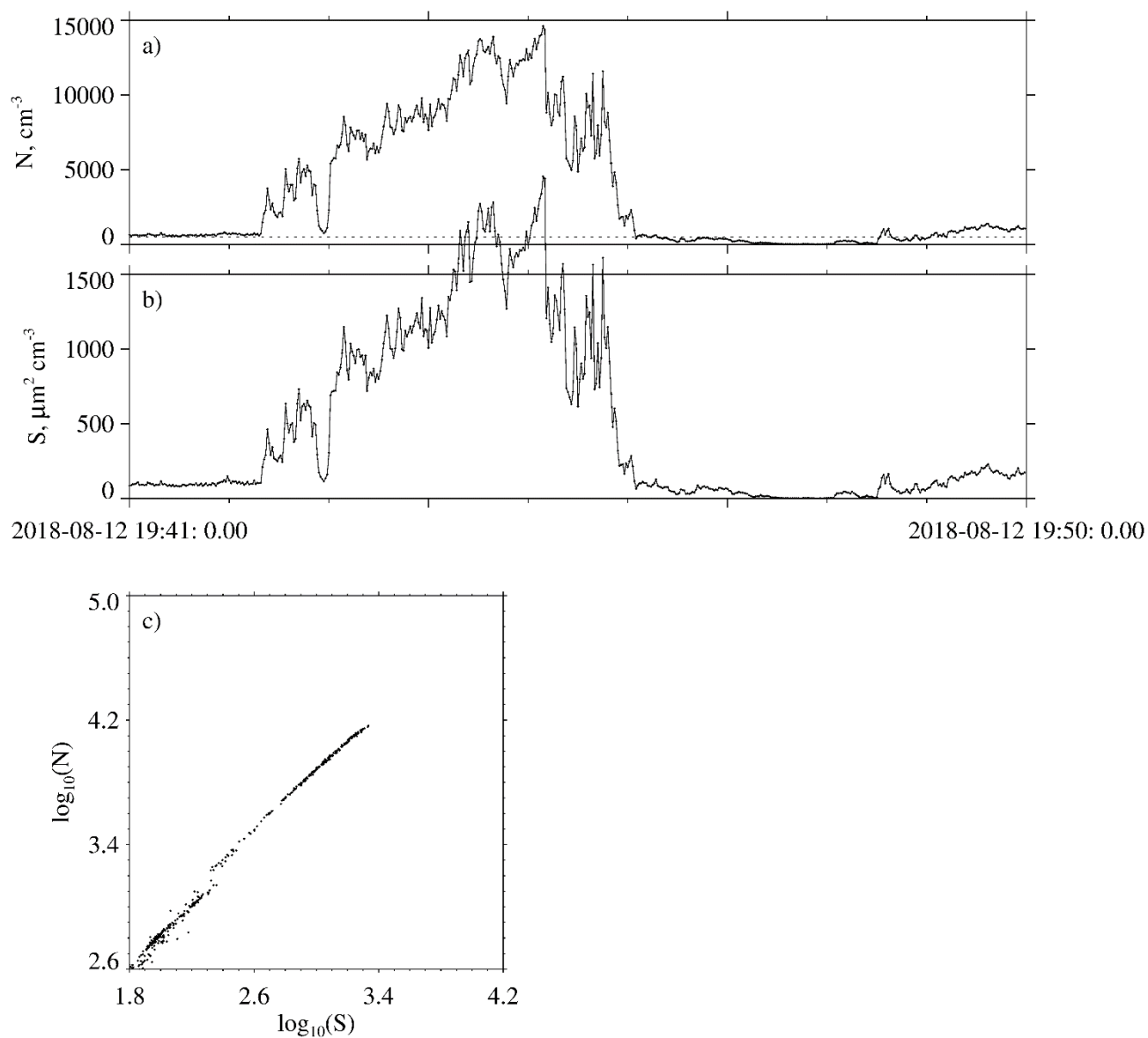


Figure 4 – Wildfire plume measurements made on 20180812 using PCASP-2. a) 9 min sequence of size-integrated aerosol concentration. b) 9 min sequence of size-integrated aerosol surface. c) N versus S scatterplot of values acquired during the 9 min sequence shown in the upper two panels.